

Keck/HIRES Spectroscopy of Four Candidate Solar Twins

Jeremy R. King

*Department of Physics and Astronomy, 118 Kinard Laboratory,
Clemson University, Clemson, SC 29634-0978*

jking2@ces.clemson.edu

Ann M. Boesgaard¹

Institute for Astronomy, 2680 Woodlawn Drive, Honolulu, HI 96822

boes@ifa.hawaii.edu

Simon C. Schuler

*Department of Physics and Astronomy, 118 Kinard Laboratory,
Clemson University, Clemson, SC 29634-0978*

sschule@ces.clemson.edu

ABSTRACT

We use high S/N, high-resolution Keck/HIRES spectroscopy of 4 solar twin candidates (HIP 71813, 76114, 77718, 78399) pulled from our *Hipparcos*-based Ca II H & K survey to carry out parameter and abundance analyses of these objects. Our spectroscopic T_{eff} estimates are some ~ 100 K hotter than the photometric scale of the recent Geneva-Copenhagen survey; several lines of evidence suggest the photometric temperatures are too cool at solar T_{eff} . At the same time, our abundances for the 3 solar twin candidates included in the Geneva-Copenhagen survey are in outstanding agreement with the photometric metallicities; there is no sign of the anomalously low photometric metallicities derived for some late-G UMa group and Hyades dwarfs. A first radial velocity determination is made for HIP 78399, and UVW kinematics derived for all stars. HIP 71813 appears to be a kinematic member of the Wolf 630 moving group (a structure apparently reidentified in a recent analysis of late-type *Hipparcos* stars), but its

¹Visiting Astronomer, W.M. Keck Observatory, jointly operated by the California Institute of Technology and the University of California.

metallicity is 0.1 dex higher than the most recent estimate of this group’s metallicity. While certainly “solar-type” stars, HIP 76114 and 77718 are a few percent less massive, significantly older, and metal-poor compared to the Sun; they are neither good solar twin candidates nor solar analogs providing a look at the Sun at some other point in its evolution. HIP 71813 appears to be an excellent solar analog of age ~ 8 Gyr. Our results for HIP 78399 suggest the promise of this star as a solar twin may be equivalent to the “closest ever solar twin” HR 6060; follow up study of this star is encouraged.

Subject headings: stars: abundances — stars: activity — stars: atmospheres — stars: evolution — stars: fundamental parameters — stars: late-type

1. Introduction

The deliberate search for and study of solar analogs has been ongoing for nearly 30 years, initiating with the seminal early works of Hardorp (e.g., Hardorp 1978). Cayrel de Strobel (1996) gives an authoritative review of this early history, many photometric and spectroscopic results, and the astrophysical motivations for studying solar analogs. As of a decade ago, these motivations were of a strong fundamental and utilitarian nature, seeking answers to such questions as: (a) what is the solar color? b) how well do photometric indices predict spectroscopic properties? c) how robust are spectral types at describing or predicting the totality of a stellar spectrum? d) are there other stars that can be used as exact photometric and/or spectroscopic proxies for the Sun in the course of astrophysical research programs?

While these important questions remain incompletely answered and of great interest, the study of solar analogs and search for solar twins has taken on renewed importance. Much of this has been driven by the detection of planetary companions around solar-type stars; the impact of these detections on solar analog research was foreshadowed with great prescience by Cayrel de Strobel (1996). Precision radial velocity searches for exoplanets are most robust when applied to slowly rotating and inactive stars; solar analogs are thus fruitful targets—metal-rich ones apparently even more fruitful (Fischer & Valenti 2005). The appeal in searching for elusive terrestrial exoplanets around solar analogs remains a natural one given the existence of our own solar system.

Solar analogs of various age also provide a mechanism to examine the past and future evolution of the Sun without significant or total recourse to stellar models. Such efforts looking at the sun in time (Ribas et al. 2005) now appear to be critical complements to studying

the evolution of planets and life surrounding solar-type stars. For example, it has been suggested that solar-type stars may be subject to highly energetic superflare outbursts, perhaps induced by orbiting planets, that would have dramatic effects on atmospheres surrounding and lifeforms inhabiting orbiting planets (Rubenstein & Schaefer 2000; Schaefer, King & Deliyannis 2000). It also seems clear that the nominal non-stochastic gradual evolution of solar-type chromospheres has important implications for a diversity of planetary physics (in our own solar system and others): the structure and chemistry of planetary atmospheres, the water budget on Mars, and even the evolution of planetary surfaces (Ribas et al. 2005); such issues are critical ones to understand in the development and evolution of life.

The utilitarian importance of studying solar analogs has also persisted. For example, there should be little argument that differential spectroscopic analyses performed relative to the Sun are most reliable when applied to stars like the Sun— early G dwarfs. Happily, such objects can be found in a large variety of stellar populations having an extreme range of metallicity and age. The development of large aperture telescopes and improved instrumentation such as multi-object spectrographs and wide field imagers over the next decade or so mean that the stellar astronomy community is poised to undertake abundance surveys of tens or hundreds of thousands of Galactic stars. Critical questions confronting such ambitious but inevitable initiatives include: a) how reliable are photometric metallicities? b) can low-resolution spectroscopy yield results as robust as those from high-resolution spectroscopy? c) will automated spectroscopic analyses needed to handle such large datasets yield reliable results? All these questions can be addressed well by comparison with the results of high-resolution spectroscopy of solar analogs.

Despite the importance of carrying out high-resolution spectroscopic analyses of solar analogs, efforts at doing so have been deliberate in pace. Recent exceptions to this include the solar analog studies of Gaidos, Henry & Henry (2000) and Soubiran & Triaud (2004). Here, we present the first results from a small contribution aimed at remedying this pace of study. Using the results of Dr. D. Soderblom’s recent chromospheric Ca II H & K survey of nearby ($d \leq 60$ pc) late-F to early-K dwarfs in the *Hipparcos* catalog, we have selected a sample of poorly-studied solar twin candidates having $0.63 \leq (B - V) \leq 0.66$, Ca II chromospheric fluxes within a few tenths of a dex of the mean solar value, and M_V within a few tenths of a magnitude of the solar value; there are roughly 150 such objects accessible from the northern hemisphere. These objects have been or are being observed as time allows during other observing programs. Here, we present echelle spectroscopy of 4 candidates obtained with Keck/HIRES. The objects are HIP 71813, 76114, 77718, and 78399.

2. Data and Analysis

2.1. Observations and Reductions

Our 4 solar twin candidates were observed on UT July 8 2004 using the Keck I 10-m, its HIRES echelle spectrograph, and a Tektronix 2048×2048 CCD detector. The chosen slit width and cross-disperser setting yielded spectra from 4475 to 6900 Å at a resolution of $R\sim 45,000$. Exposure times ranged from 3 to ~ 6 minutes, achieving per pixel S/N in the continuum near 6707 Å of ~ 400 . A log of the observations containing cross-identifications is presented in Table 1. Standard reductions were carried out including debiasing, flat-fielding, order identification/tracing/extraction, and wavelength calibration (via solutions calculated for an internal Th-Ar lamp). The H α and H β features are located at the blue edge of their respective orders; the lack of surrounding wavelength coverage with which to accomplish continuum normalization thus prevented us from using Balmer profile fitting to independently determine T_{eff} . Samples of the spectra in the $\lambda 6707$ Li I region can be found later in Figures 3 and 4.

Tab. 1

2.2. Parameters and Abundances

Clean, “case a” Fe I and Fe II lines from the list of Thevenin (1990) were selected for measurement in our 4 solar twin candidate spectra and a similarly high S/N and $R\sim 45,000$ Keck/HIRES lunar spectrum (described in King et al. (1997)) used as a solar proxy spectrum. Equivalent widths were measured using the profile fitting routines in the 1-d spectrum analysis software package SPECTRE (Fitzpatrick & Sneden 1987). Line strengths of all the features measured in each star and our solar proxy spectrum can be found in Table 2. Abundances were derived from the equivalent widths using the 2002 version of the LTE analysis package MOOG and Kurucz model atmospheres interpolated from ATLAS9 grids. Oscillator strengths were taken from Thevenin (1990); the accuracy of these is irrelevant inasmuch as normalized abundances $[x/H]$ were formed on a line-by-line basis using solar abundances derived in the same manner. The solar model atmosphere was characterized by $T_{\text{eff}} = 5777$ K, $\log g = 4.44$, a metallicity of $[m/H]=0.$, and a microturbulent velocity of $\xi = 1.25$; the latter is intermediate to the values of ξ from the calibrations of Edvardsson et al. (1993) and Allende Prieto et al. (2004). An enhancement factor of 2.2 was applied to the van der Waals broadening coefficients for all lines.

Tab. 2

Stellar parameters were determined as part of the Fe analysis in the usual fashion. T_{eff} and ξ were determined by requiring zero correlation coefficient between the *solar normalized* abundances (i.e., $[Fe/H]$; again, accomplished on a line-by-line basis) and the lower excita-

tion potential and reduced equivalent width, respectively. This approach leads to unique solutions when there is no underlying correlation between excitation potential and reduced equivalent width. We show in Figure 1 that there is no such underlying correlation in our Fe I sample. Figure 2 displays the Fe I-based line-by-line $[\text{Fe}/\text{H}]$ values versus both lower excitation potential (top) and reduced equivalent width (bottom) using our final model atmosphere parameters for the case of HIP 76114; the linear correlation coefficients in both planes are ~ 0.00 . Our abundance analysis is thus a purely differential one, and the derived parameters do not depend on the rigorous accuracy of the gf values. The 1σ level uncertainties in T_{eff} and ξ were determined by finding the values of these parameters where the respective correlation coefficients became significant at the 1σ confidence level. Gravity estimates were made via ionization balance of Fe. The error estimates for $\log g$ include uncertainties in both $[\text{Fe I}/\text{H}]$ and $[\text{Fe II}/\text{H}]$ due to measurement uncertainty, T_{eff} errors, and ξ errors. The final parameters and their uncertainties can be found in the summary of results in Table 4.

Fig. 1
Fig. 2

Abundances of Al, Ca, Ti, and Ni were derived in a similar fashion using the line data in Table 2 and model atmospheres characterized by the parameters determined from the Fe data. Abundances of a given species were normalized on a line-by-line basis using the values derived from the solar spectrum, and then averaged together. Typical errors in the mean are only 0.01-0.02 dex, indicative of the quality of the data. The sensitivity of the derived abundances to arbitrarily selected fiducial variations in the stellar parameters (± 100 K in T_{eff} ; ± 0.2 dex in $\log g$; and ± 0.2 km s $^{-1}$ in microturbulence) are provided for each element in Table 3. Coupling these with the parameter uncertainties and the statistical uncertainties in the mean yielded total uncertainties in the abundance ratio of each element. The mean abundances and the 1σ uncertainties are given in Table 4.

Tab. 3
Tab. 4

2.3. Oxygen Abundances

O abundances were derived from the measured equivalent widths of the $\lambda 6300$ [O I] feature (Table 2) using the `blends` package in `MOOG` to account for contamination by a Ni I feature at 6300.34. Isotopic components (Johansson et al. 2003) of Ni were taken into account with the gf values taken from Bensby, Feltzing & Lundstrom (2004); the [O I] gf value (-9.717) is taken from Allende Prieto, Lambert, & Asplund (2001). The assumed Ni abundances were taken as $[\text{Ni}/\text{H}] = 0.00, -0.04, -0.16,$ and -0.01 for HIP 71813, 76114, 77718, and 78399 respectively. Abundances are given in Table 4. Uncertainties in $[\text{O}/\text{H}]$ are dominated by those in the equivalent widths (0.5 mÅ) measurements of the stars and the Sun, and that in $\log g$ (0.12 dex). These uncertainties from these 3 sources were added in

quadrature to yield the total uncertainties associated with the [O/H] values given in Table 4.

2.4. Lithium Abundances

Li abundances were derived from the $\lambda 6707$ Li I resonance features via spectrum synthesis. Utilizing the derived parameters, synthetic spectra of varying Li abundance were created in MOOG using the line list from King et al. (1997). No contribution from ${}^6\text{Li}$ was assumed, a reasonable assumption given that the Li abundances in our objects are well-below meteoritic ($\log N(\text{Li})=3.31$; ${}^6\text{Li}/{}^7\text{Li}= 0.08$). Smoothing was carried out by convolving the synthetic spectra with Gaussians having FWHM values measured from clean, weak lines measured in our spectra. Comparison of the syntheses (solid lines) and the Keck/HIRES spectra in the $\lambda 6707$ region are shown in Figures 3 and 4. Total uncertainties include those due to uncertainties in the T_{eff} value (Table 3) and in the fit itself. The Li results are listed in Table 4.

Fig. 3
Fig. 4

2.5. Rotational Velocity and Chromospheric Emission

The same FWHM values measured for each star and used to smooth the syntheses were assumed to be the quadrature sum of components due to spectrograph resolution and (twice the projected) rotational velocity. The resulting $v \sin i$ values are listed in Table 4. Inasmuch as we assume no contribution from macroturbulent broadening mechanisms, we present these estimates as upper limits to the projected rotational velocity. The Ca II H&K chromospheric emission indices of our objects are listed in Table 4 and come from the low-resolution ($R\sim 2000$) KPNO coude' feed-based survey of D. Soderblom.

2.6. Masses and Ages

Masses and ages of the Sun and our four solar twin candidates were estimated by placing them in the M_V versus T_{eff} plane using our temperature estimates and the Hipparcos-based absolute visual magnitudes. Comparison of these positions with isochrones and sequences of constant mass taken from appropriate metallicity Yonsei-Yale Isochrones (Yi, Kim & Demarque 2003) (as updated by Demarque et al. (2004)) yielded the mass and age estimates in Table 4. The uncertainties in mass and age are calculated assuming the influence of uncertainties in our T_{eff} and M_V values; including the uncertainty in our metallicity esti-

mates ($\sigma \sim 0.04$ dex) has a negligible effect on the uncertainty of our estimated masses, but would contribute an additional 0.4 Gyr uncertainty in the age estimates. The HR diagrams containing our objects and these isochrones are shown in Figure 5.

Fig. 5

3. Results and Discussion

3.1. Comparison with Previous Results

HIP 71813 is included in the recent Geneva-Copenhagen solar neighborhood survey of Nordstrom et al. (2004). Their photometric metallicity determination of $[\text{Fe}/\text{H}] = +0.01$ is in outstanding agreement with our Al, Ca, Ti, Fe, and Ni abundances, which range from -0.02 to $+0.02$. Their photometric T_{eff} estimate of 5662 K is some 90 K lower than our spectroscopic value. If the solar color, $(B - V)_{\odot} = 0.642$, adopted in Table 4 is to be believed, then our T_{eff} value would seem to be more consistent with the nearly indistinguishable $(B - V)$ index (0.644) of HIP 71813.

HIP 76114 is also included in the Geneva-Copenhagen survey. The Nordstrom et al. (2004) photometric metallicity of $[\text{Fe}/\text{H}] = -0.05$ is also in outstanding agreement with our Al, Ca, Ti, Fe, and Ni abundances, which range from -0.06 to -0.02 . The photometric T_{eff} difference between HIP 71813 and 76114 (former minus latter) of 52 K is in excellent agreement with our spectroscopic difference of 40 K.

HIP 77718 has a photometric metallicity, $[\text{Fe}/\text{H}] = -0.19$ from the Nordstrom et al. (2004) solar neighborhood survey that is in good agreement with our Al, Ti, Fe, and Ni determinations, which range from -0.15 to -0.22 ; our $[\text{Ca}/\text{H}]$ abundance of -0.09 appears only mildly anomalous in comparison. The HIP 77718 minus 71813 photometric T_{eff} difference of 92 K is in outstanding agreement with the 90 K spectroscopic difference. Gray et al. (2003) have determined the parameters and overall abundance of HIP 77718 via the analysis of low resolution blue spectra as part of their NStar survey. The independent spectroscopic T_{eff} estimate, made via different comparisons of different spectral features in a different part of the spectrum, of 5859 K is only 19 K larger than our own and 105 K larger than the photometric value. The Gray et al. (2003) metallicity of $[\text{m}/\text{H}] = -0.15$ is indistinguishable from our own result.

HIP 78399 has not been subjected to any published abundance or high-resolution spectroscopic analysis that we are aware of. Accordingly, it lacks a radial velocity determination. We remedied this by determining a radial velocity relative to HIP 76114 via cross-correlation of the spectra in the 6160-6173 Å range. We assumed the precision radial velocity of -35.7 km/s from Nidever et al. (2002) for HIP 76114. Cross-correlation of the telluric B-Band

spectra in the 6880 Å region revealed a 9.9 km/s offset between the spectra. While larger than anticipated, this intra-night drift was confirmed by comparison of telluric water vapor features in the 6300 Å region. Accounting for this drift and the appropriate relative heliocentric corrections, we find a radial velocity of -24.7 ± 0.7 km/s for HIP 78399.

3.2. HIP 71813 and the Wolf 630 Moving Group

Eggen (1969) included HIP71813 as a member of the Wolf 630 moving group. Membership in this putative kinematic population was defined by Eggen in a vast series papers as traced in the work of McDonald & Hearnshaw (1983). Regardless of one’s view on the reality of these kinematic assemblages, it is likely that the recent passing of O. Eggen has meant that a wealth of modern data (in particular *Hipparcos* parallaxes and precision radial velocities) has not yet been brought to bear on the reality, properties, and detailed membership of the Wolf 630 group. A notable exception is the work of Skuljan, Hearnshaw & Cottrell (1999), who find a clustering of late-type stars at $(U, V) = (+20, -30)$ km s⁻¹ that is absent in the kinematic phase space of their early-type stellar sample; this is highly suggestive of an old moving group at Eggen’s suggested position of the Wolf 630 group in the Bottlinger (U, V) diagram. The salient characteristics identified by Eggen for the Wolf 630 group are a) a kinematically old disk population, b) a characteristic Galactic rotational velocity of $V = -33$ km/s, and c) a color-luminosity array similar to M 67.

It is beyond the scope of this paper to revisit or refine characteristics of the Wolf 630 group. However, several notes can be made. First, our 8 Gyr age estimate for HIP 71813 is certainly consistent with an old disk object. Second, if the estimate of Taylor (2000) of $[\text{Fe}/\text{H}] = -0.12$ for the Wolf 630 group metallicity is accurate, then HIP 71813 would not seem to be a member. Third, using *Hipparcos* parallaxes and proper motions, and modern radial velocity determinations (Nordstrom et al. 2004; Tinney & Reid 1998), the UVW kinematics of HIP 71813 can be compared with those of Wolf 629, a Wolf 630 group defining member according to Eggen. The heliocentric Galactic velocities of all our objects are listed in Table 4. The $(U, V) = (+21.3 \pm 1.5, -36.3 \pm 1.3)$ results for HIP 71813 are in excellent agreement with those for Wolf 629 $(+21.0 \pm 1.3, -33.4 \pm 1.0)$, and consistent with the canonical Wolf 630 group values (26, -33) given by Eggen (1969). None of our other candidate solar twins has kinematics, which are listed in Table 4, consistent with those of the Wolf 630 group.

3.3. Solar Twin Status Evaluation

HIP 71813. The T_{eff} value, light metal-abundances, and chromospheric Ca II emission of HIP 71813 are indistinguishable from solar values. The Li abundance, however, appears to be depleted by a factor of ≥ 2 compared to the Sun. More importantly, however, the star appears significantly more evolved than the sun. The M_V and $\log g$ values are significantly lower than the solar values, and our estimated age is a factor of 2 older than the Sun’s. While clearly an inappropriate solar twin candidate, the star would appear to be an excellent solar analog of significantly older age.

HIP 76114. HIP 76114 is marginally cooler than the Sun, $\Delta T_{\text{eff}} = -67$ K. While any of the light element abundances alone are indistinguishable from solar, taken together they suggest a metallicity some 0.04 dex lower than solar; this is confirmed by the photometric metallicity of Nordstrom et al. (2004). The Ca II emission and Li abundance is solar within the uncertainties, but the star appears marginally evolved relative to the Sun as indicated by its slightly lower M_V and $\log g$ values; table 4 suggests that HIP 76114 is ≥ 1.5 Gyr older than the Sun. This object may be a suitable solar analog of slightly older age, albeit of likely slightly lower metallicity, that can be included in studies looking at solar evolution.

HIP 77718. While the Ca II chromospheric emission and age determination of HIP 77718 are observationally indistinguishable from the Sun, our analysis indicates this star is clearly warmer ($\Delta T_{\text{eff}} = 63$ K) and some 0.16 dex metal-poor relative to solar; both the warmer temperature and slightly metal-poor nature are independently confirmed by the spectroscopic analysis of Gray et al. (2003). The Li abundance is some 20 times higher than solar. This difference may be related to reduced PMS Li depletion due to lower metallicity or reduced main-sequence depletion due to a younger age; our observations can not distinguish between these possibilities. Regardless, this star is not a good solar twin candidate, nor an optimal metal-poor or younger solar analog.

HIP 78399. The poorly-studied HIP 78399 appears to hold great promise as a solar twin candidate. Its T_{eff} , luminosity, mass, age, light metal abundances, and rotational velocity are all indistinguishable from solar values. The only marked difference seen is the Li abundance, which is a factor of ~ 6 larger than the solar photospheric abundance. While the evolution of Li depletion in solar-type stars is a complex and still incompletely understood process subject to vigorous investigation, this difference may suggest a slightly younger age for HIP 78399, which is allowed by our age determination and may be consistent with a slightly larger Ca II chromospheric flux.

Currently, the “closest ever solar twin” title belongs to HR 6060 (Porto De Mello & Da Silva 1997). Several spectroscopic analyses of this star have been carried out (Luck & Heiter

2005; Allende Prieto et al. 2004; Gray et al. 2003; Porto De Mello & Da Silva 1997). T_{eff} estimates range from 5693 to 5835 K, and $[\text{Fe}/\text{H}]$ estimates from -0.06 to $+0.05$; the precision T_{eff} analysis using line ratios (Gray 1995) indicates a T_{eff} difference with respect to the Sun of 17 K. The Ca II H&K emission index (-5.00 , Gray 1995) and rotational velocity (≤ 3 km/s, De Mello & Da Silva 1997) are indistinguishable from solar values. The *Hipparcos*-based absolute magnitude strongly suggests the mass and age of HR 6060 are virtually identical to the Sun’s (Porto De Mello & Da Silva 1997). Just as for HIP 78399, the only glaring outlying parameter is Li abundance, which is a factor of ~ 4 larger than the solar photospheric Li abundance (Stephens 1997). The work of Jones, Fischer & Soderblom (1999) on $1 M_{\odot}$ stars in the solar-age and -abundance cluster M67 suggests that we can expect such objects to exhibit a ~ 1 dex range in Li; thus, the Sun may not be an especially good Li ”standard”.

Based on our analysis, we believe there is a case to be made that HIP 78399 share the stage with HR 6060 as the closest ever solar twin. For those engaged in studies of solar twins or the Sun in time, HIP 78399 is certainly worthy of closer follow-up study. Particularly valuable would be: a) refining its T_{eff} and luminosity estimates relative to the Sun via Balmer line profile fitting, analysis of line ratios, etc. b) analysis of the $\lambda 7774$ O I lines to confirm whether its O abundance is truly subsolar, c) performing an independent check on its relative age via the $[\text{Th}/\text{Nd}]$ ratio (Morell, Kallander, & Butcher 1992), and d) determining a ${}^9\text{Be}$ abundance, which is more immune to the effects of stellar depletion and also contains embedded information about the “personal” integrated Galactic cosmic-ray history of matter comprised by the star.

4. Summary

We have carried out high S/N high-resolution Keck/HIRES spectroscopy of four candidate solar twins drawn from a *Hipparcos*-defined Ca II H&K survey. Parameters, abundances, masses, ages, and kinematics have been derived in a differential fine analysis. Comparisons suggests that the *relative* photometric T_{eff} values of Nordstrom et al. (2004) and our spectroscopic temperatures are indistinguishably robust; however, the photometric T_{eff} values are typically 100 K cooler. There are several lines of evidence that suggest the photometric scale is misanchored (at least near solar T_{eff}). First, if the solar color of Cayrel de Strobel (1996) is nearly correct, then our spectroscopic T_{eff} values are in outstanding accord with the colors of HIP 71813 and 78399. Second, the independent analysis of HIP 77718 by Gray et al. (2003) using different spectral features in the blue yields a spectroscopic T_{eff} in outstanding agreement with our own. Third, the Nordstrom et al. (2004) photometric T_{eff} estimate for the “closest ever solar twin” HR 6060 is 5688 K, some 100 K lower than the precision T_{eff}

estimate of Gray (1995).

At the same time, our light metal-abundances are in excellent agreement with the photometric metallicity estimates for the 3 of our objects in Nordstrom et al. (2004), differing by no more than a few hundredths of a dex. There is no sign of the abnormally low photometric metallicity values seen for some very cool Pop I dwarfs in the Hyades and UMa group as noted by King & Schuler (2005). As these authors note, anomalous photometric estimates may be restricted to late G dwarfs. Our spectroscopic metallicity for HIP 77718 is in nearly exact agreement with that derived from low-resolution blue spectra by Gray et al. (2003).

We present the first abundances and radial velocity estimate for HIP 78399. Using the radial velocities and *Hipparcos* proper motions and parallaxes, we derive the UVW kinematics of our four solar twin candidates. The position of HIP 71813 in the (U, V) plane is consistent with membership in Eggen’s Wolf 630 moving group, a kinematic structure of late-type *Hipparcos* stars apparently verified by Skuljan, Hearnshaw & Cottrell (1999). Our metallicity for HIP 71813, $[Fe/H] = -0.02$, is 0.1 dex higher than the Wolf 630 estimate of Taylor (2000), however. Revisiting the characteristic metallicity via identification of assured Wolf 630 group members using *Hipparcos* data and new precision radial velocities, and follow-up high resolution spectroscopy to determine abundances would be of great value.

HIP 77718 is ~ 70 K warmer than the Sun, significantly more metal-poor ($[m/H] \sim -0.16$), significantly more Li-rich ($\log N(\text{Li}) \sim 2.3$) and a few percent less massive than the Sun; we deem it neither a suitable solar twin nor solar analog to trace the evolution of the Sun. The light-metal and Li abundances of HIP 76114 are much closer to solar. However, HIP 76114 does appear to be slightly metal-poor ($[m/H] = -0.04$), cooler $\Delta T_{\text{eff}} = 67$ K, older $\Delta \tau \geq 3$ Gyr, and a few percent less massive compared to the Sun.

HIP 71813 appears to be an excellent solar analog of solar abundance, mass, and T_{eff} , but advanced age– $M_V = 4.45$ and $\tau \sim 8$ Gyr; the more evolved state of this star is likely reflected in the subsolar upper limit to its Li abundance. Finally, our first ever analysis of HIP 78399 suggests this object may be a solar twin candidate of quality comparable to the “closest ever solar twin” HR 6060 (Porto De Mello & Da Silva 1997). The T_{eff} , mass, age, and light metal abundances of this object are indistinguishable from solar given the uncertainties. The only obvious difference is that which characterizes HR 6060 as well– a Li abundance a factor of a few larger than the solar photospheric value. This object merits additional study as a solar twin to refine its parameters; of particular interest will be confirming our subsolar O abundance derived from the very weak $\lambda 6300$ [O I] feature.

We are indebted to Dr. David Soderblom for the use of his nearby star activity catalog from which our objects were selected and for his valuable comments on the manuscript. It is a

pleasure to thank Dr. M. Novicki for her careful and cheerful help in the Keck data reduction. JRK gratefully acknowledges support for this work from NSF awards AST-0086576 and AST-0239518, and a generous grant from the Charles Curry Foundation to Clemson University. Additional support was provided by NSF award AST-0097955 to AMB. SCS was supported by a graduate scholarship from the South Carolina Space Grant Consortium.

REFERENCES

- Allende Prieto, C., Lambert, D. L., & Asplund, M. 2001, *ApJ*, 556, L63
- Allende Prieto, C., Barklem, P. S., Lambert, D. L., & Cunha, K. 2004, *A&A*, 420, 183
- Bensby, T., Feltzing, S., & Lundstrom, I. 2004, *A&A*, 415, 155
- Cayrel de Strobel, G. 1996, *A&ARv*, 7, 243
- Demarque, P., Woo, J.-H., Kim, Y.-C., & Yi, S. K. 2004, *ApJS*, 155, 667
- Edvardsson, B., Andersen, J., Gustafsson, B., Lambert, D. L., Nissen, P. E., & Tomkin, J. 1993, *A&A*, 275, 101
- Eggen, O. J. 1969, *PASP*, 81, 553
- Fischer, D. A., & Valenti, J. 2005, *ApJ*, 622, 1102
- Fitzpatrick, M. J., & Sneden, C. 1987, *BAAS*, 19, 1129
- Gaidos, E. J., Henry, G. W., & Henry, S. M. 2000, *AJ*, 120, 1006
- Gray, R. O., Corbally, C. J., Garrison, R. f., McFadden, M. T., & Robinson, P. E. 2003, *AJ*, 126, 2048
- Gray, D. F. 1995, *PASP*, 107, 120
- Hardorp, J. 1978, *A&A*, 63, 383
- Johansson, S., Litzen, U., Lundberg, H., & Zhang, Z. 2003, *ApJ*, 584, L107
- Jones, B. F., Fischer, D., & Soderblom, D. R. 1999, *AJ*, 117, 330
- King, J. R., Deliyannis, C. P., Hiltgen, D. D., Stephens, A., Cunha, K., & Boesgaard, A. M. 1997, *AJ*, 113, 1871
- King, J. R. & Schuler, S. C. 2005, *PASP*, in press

- Luck, R. E., & Heiter, U. 2005, *AJ*, 129, 1063
- McDonald, A. R. E., & Hearnshaw, J. B. 1983, *MNRAS*, 204, 841
- Morell, O., Kallander, D., & Butcher, H. R. 1992, *A&A*, 259, 543
- Nidever, D. L., Marcy, G. W., Butler, R. P., Fischer, D. A., Vogt, S. S. 2002, *ApJS*, 141, 503
- Nordstrom, B., Mayor, M., Andersen, J., Holmberg, J., Pout, F., Jorgensen, B. R., Olsen, E. H., Udry, S., & Mowlavi, N. 2004, *A&A*, 418, 989
- Porto De Mello, G. F., & Da Silva, L. 1997, *ApJ*, 482, L89
- Ribas, I., Guinana, E. f., Guden, M., & Audard, M. 2005, *ApJ*, 622, 680
- Rubenstein, E. P., & Schaefer, B. E. 2000, *ApJ*, 529, 1031
- Schaefer, B. E., King, J. R., & Deliyannis, C. P. 2000, *ApJ*, 529, 1026
- Skuljan, J., Hearnshaw, J. B., & Cottrell, P. L. 1999, *MNRAS*, 308, 731
- Soubiran, C., & Triaud, A. 2004, *A&A*, 418, 1089
- Stephens, A. 1997, *ApJ*, 491, 339
- Taylor, B. J. 2000, *A&A*, 362, 563
- Thevenin, F. 1990, *A&AS*, 82, 179
- Tinney, C. G., & Reid, I. N. 1998, *MNRAS*, 301, 1031
- Yi, S. K., Kim, Y.-C., & Demarque, P. 2003, *ApJS*, 144, 259

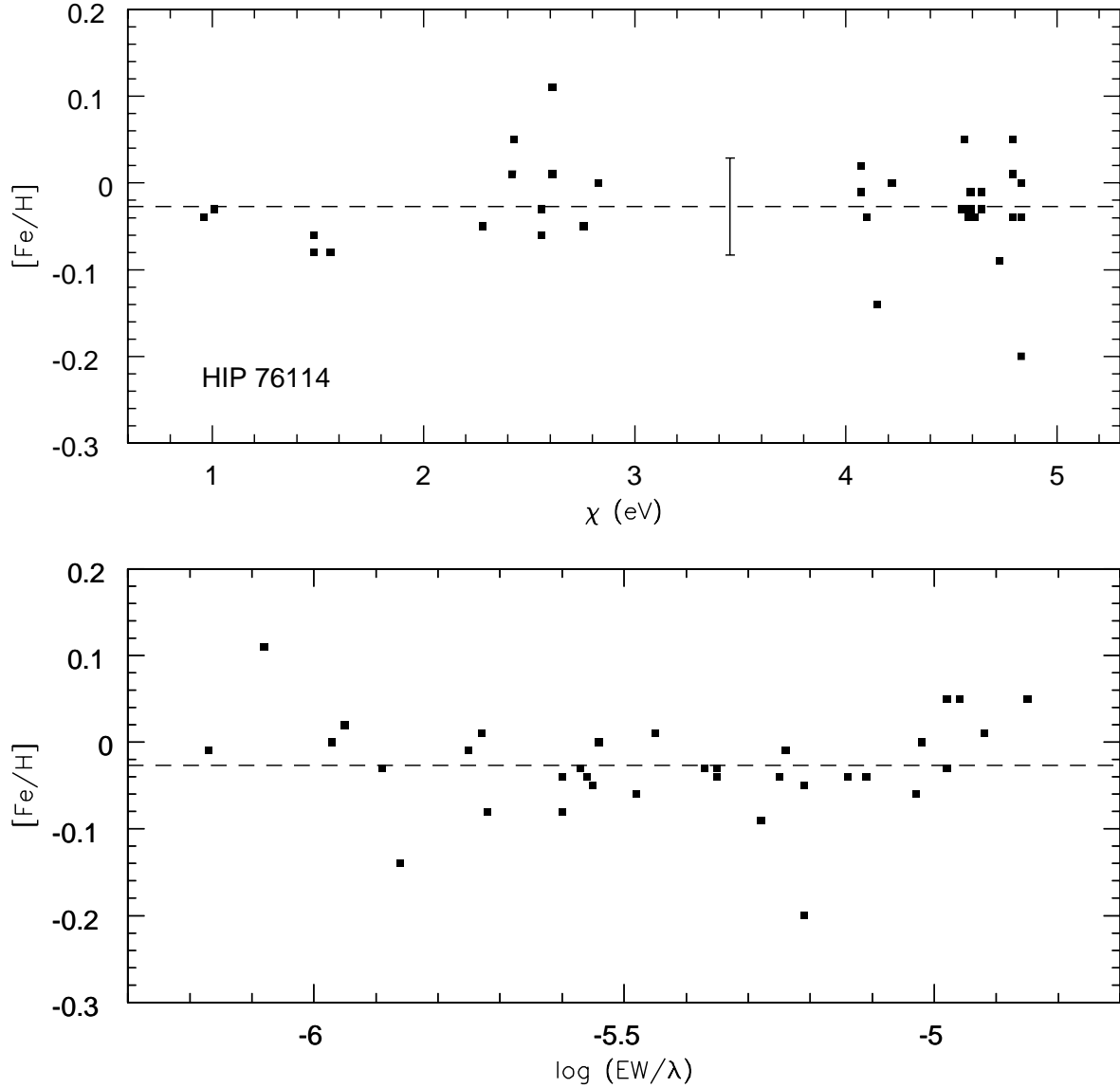


Fig. 2.— (Top) The HIP 76114 line-by-line Fe I-based $[Fe/H]$ abundances with our final model atmosphere parameters are shown versus lower excitation potential. The error bar shows the line-to-line scatter (not the mean uncertainty). (Bottom) The same $[Fe/H]$ abundances are shown versus reduced equivalent width. The linear correlation coefficients in both panel are ~ 0.00 .

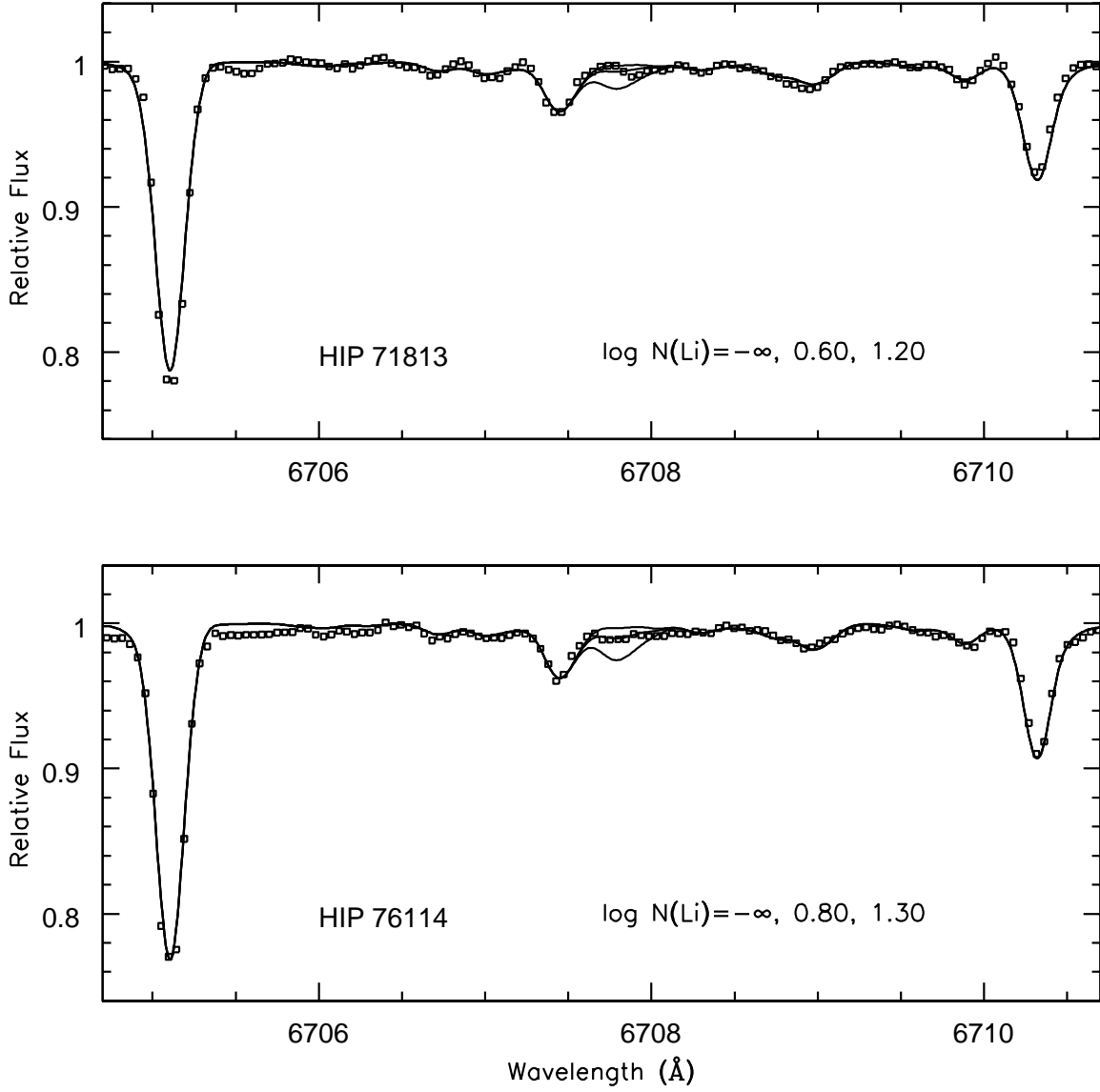


Fig. 3.— The $\lambda 6707$ Li I region Keck/HIRES spectra (open squares) of HIP 71813 (top) and HIP 76114 (bottom) are shown with syntheses of varying Li abundance (solid lines).

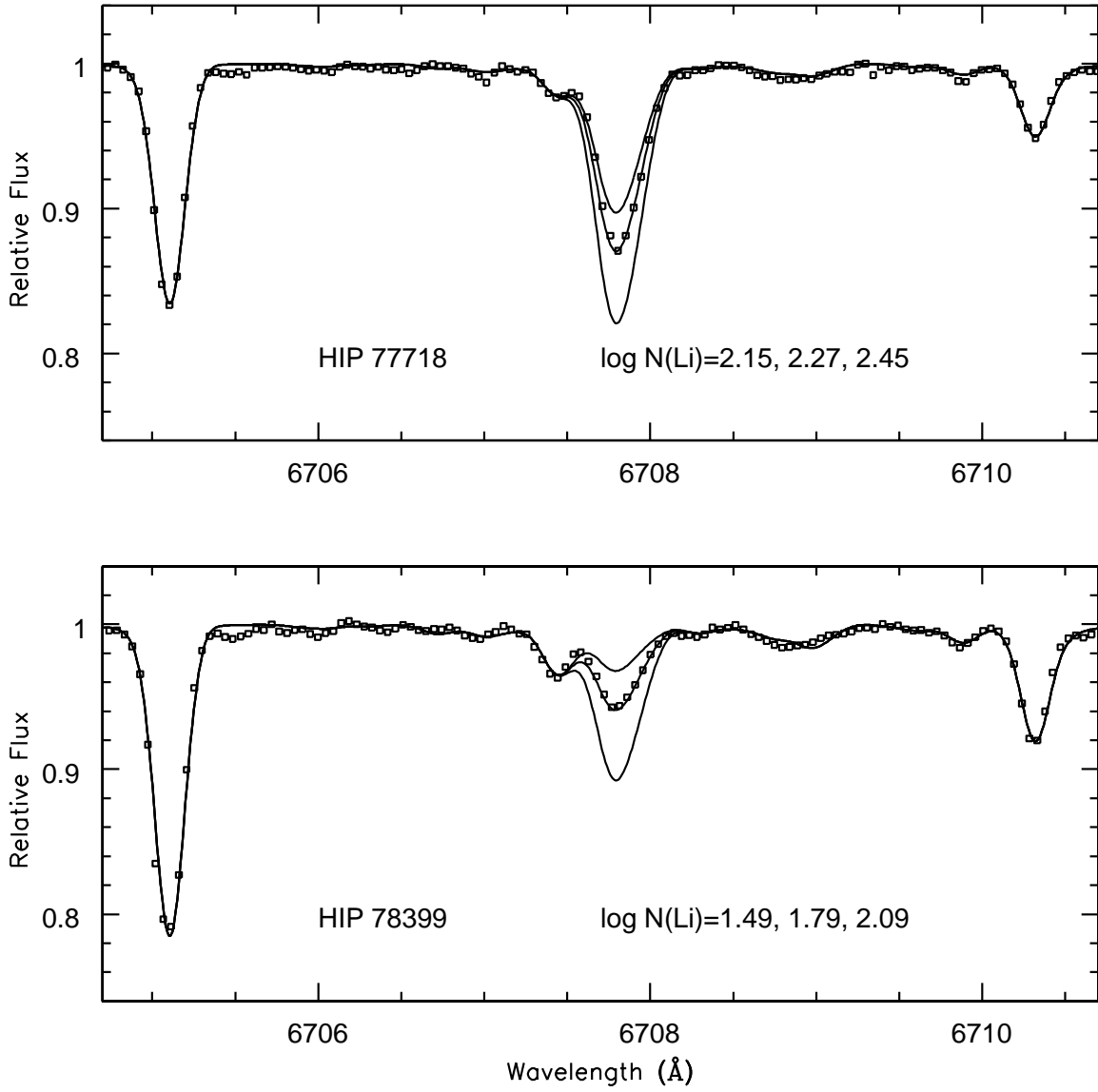


Fig. 4.— Same as Figure 2 for HIP 77718 (top) and HIP 78399 (bottom).

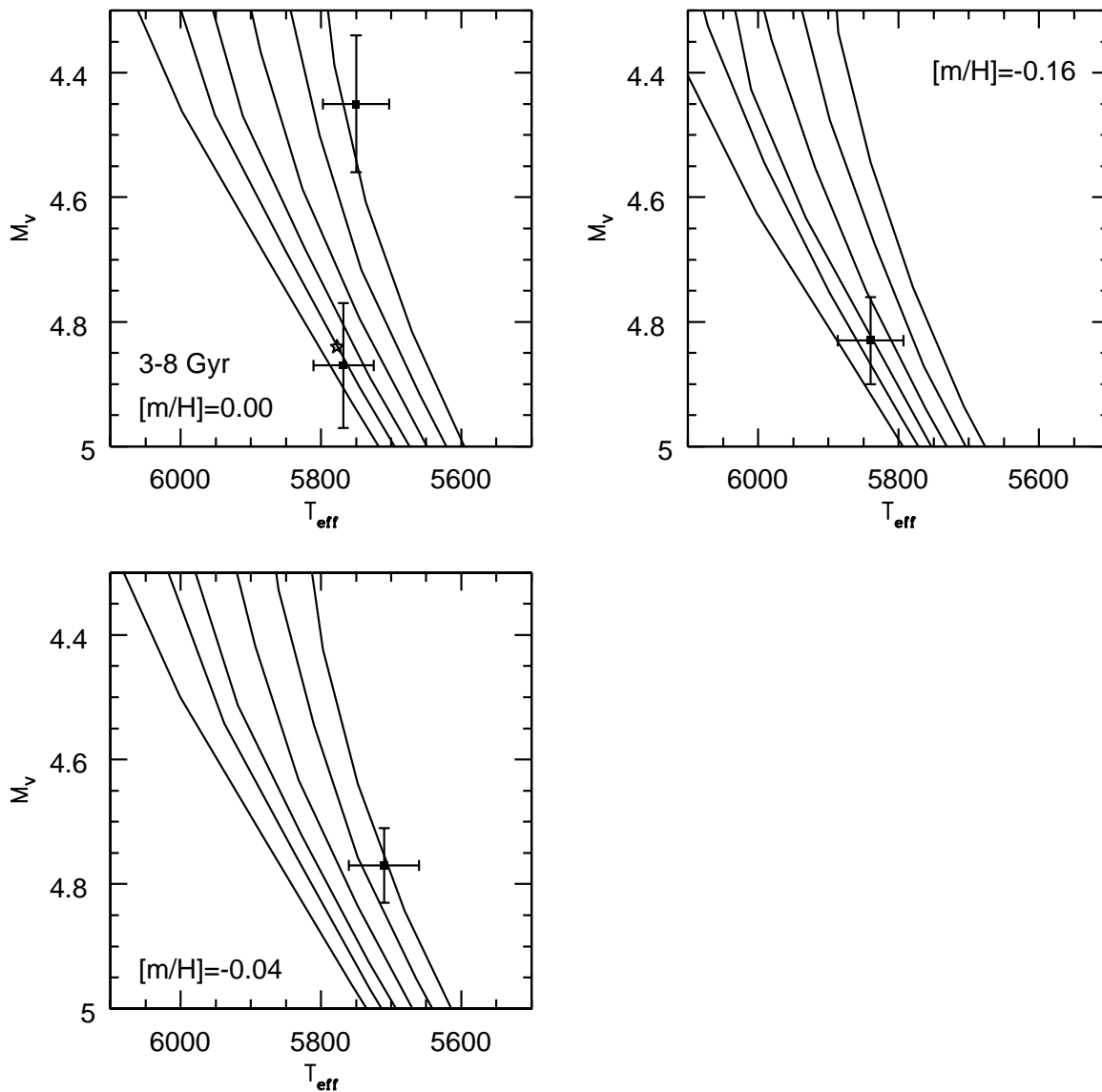


Fig. 5.— The Yale-Yonsei evolutionary tracks for 3-8 Gyr for $[\text{Fe}/\text{H}]=0.00$ (upper left), -0.04 (lower left), and -0.16 (upper right) are plotted with our 4 candidate solar analogs, whose locations are defined by our spectroscopic temperatures and the *Hipparcos*-based absolute magnitudes. The $[m/H]=0.00$ (upper left) plane contains HIP 71813 and 78399 and the Sun (open star). The $[m/H]=-0.16$ (upper right) plane contains HIP 77718. The $[m/H]=-0.04$ plane (lower left) plane contains HIP 76114.

Table 1. Observational Log

HIP #	HD #	V	exp. (s)	S/N
71813	129357	7.82	382	456
76114	138573	7.23	180	381
77718	142093	7.32	180	383
78399	143436	8.06	300	363

Table 2. Line Data

Species	λ Å	χ eV	$\log gf$	EW(Sun) mÅ	$\log N$	EW(HIP71813) mÅ	$\log N$	EW(HIP76114) mÅ	$\log N$	EW(HIP77718) mÅ	$\log N$	EW(HIP78399)	$\log N$
O I	6300.3	0.00	-9.72	5.5 ^a	8.69	7.3	8.72	7.5	8.76	2.8	8.18	4.8	8.47
Al I	6696.03	3.14	-1.65	40.3	6.61	41.1	6.62	39.8	6.57	25.8	6.38	36.8	6.55
	6698.67	3.14	-1.95	23.2	6.58	22.7	6.56	23.0	6.54	15.4	6.40	20.2	6.50
Ca I	6455.60	2.52	-1.50	59.7	6.47	60.2	6.50	59.5	6.43	48.9	6.36	59.1	6.46
	6464.68	2.52	-2.53	13.3	6.53	14.1	6.54	13.9	6.51	10.1	6.44	13.6	6.53
	6499.65	2.52	-1.00	89.8	6.45	87.4	6.46	91.5	6.45	79.7	6.38	94.6	6.53
Ti I	6599.11	0.90	-2.06	10.2	5.01	11.1	5.03	10.5	4.95	6.3	4.85	10.8	5.03
Fe I	6475.63	2.56	-2.97	60.1	7.63	54.4	7.51	61.0	7.57	45.6	7.44	59.5	7.60
	6481.88	2.28	-3.01	64.1	7.47	63.9	7.46	53.5	7.36	64.2	7.45
	6494.50	4.73	-1.44	37.1	7.78	32.3	7.67	34.4	7.69	24.2	7.54	35.4	7.74
	6495.74	4.83	-1.11	49.8	7.77	37.8	7.55	40.3	7.57	30.5	7.45	42.5	7.63
	6496.47	4.79	-0.65	63.7	7.51	60.5	7.47	68.7	7.56	55.3	7.42	64.0	7.51
	6498.94	0.96	-4.70	46.2	7.49	45.4	7.44	49.9	7.45	34.0	7.34	47.6	7.49
	6509.61	4.07	-2.97	4.1	7.51	4.5	7.53	4.4	7.50	2.7	7.36	4.3	7.52
	6518.37	2.83	-2.67	58.0	7.56	56.7	7.52	62.0	7.56	45.9	7.41	60.7	7.59
	6581.22	1.48	-4.82	21.0	7.61	21.7	7.59	21.8	7.55	12.9	7.41	19.6	7.55
	6591.33	4.59	-2.07	11.0	7.57	9.7	7.49	11.7	7.56	8.6	7.49	10.1	7.52
	6593.88	2.43	-2.34	86.6	7.36	87.3	7.39	94.2	7.41	76.8	7.29	90.3	7.41
	6608.04	2.28	-4.02	17.9	7.52	17.6	7.48	18.7	7.47	11.9	7.36	18.0	7.50
	6609.12	2.56	-2.67	66.2	7.43	69.1	7.49	68.7	7.40	55.8	7.32	69.2	7.47
	6625.04	1.01	-5.38	16.3	7.55	15.8	7.50	17.9	7.52	9.7	7.36	16.8	7.55
	6627.56	4.55	-1.59	28.6	7.58	28.9	7.57	29.3	7.55	20.2	7.41	29.5	7.59
	6633.43	4.83	-1.35	29.8	7.63	30.2	7.63	29.9	7.59	21.2	7.46	31.1	7.65
	6633.76	4.56	-0.79	67.2	7.49	64.7	7.47	72.1	7.54	58.5	7.41	71.7	7.57
	6634.12	4.79	-1.32	37.7	7.72	37.4	7.71	37.3	7.68	26.8	7.53	36.6	7.69
	6646.97	2.61	-4.01	10.8	7.57	9.7	7.49	12.4	7.58	6.2	7.36	10.1	7.52
	6653.91	4.15	-2.53	11.2	7.61	9.7	7.52	9.2	7.47	6.8	7.41	8.5	7.47
	6696.32	4.83	-1.65	18.1	7.64	20.4	7.69	19.4	7.64	13.4	7.51	17.6	7.61
	6699.14	4.59	-2.22	8.5	7.59	8.7	7.59	8.6	7.56	6.1	7.47	8.7	7.59
	6703.58	2.76	-3.13	40.0	7.60	39.2	7.57	41.0	7.55	28.7	7.43	38.5	7.56
	6704.50	4.22	-2.67	6.5	7.56	5.5	7.46	7.2	7.56	5.5	7.52	8.3	7.67
	6710.32	1.48	-4.90	16.8	7.56	15.8	7.49	16.9	7.48	10.2	7.37	16.7	7.54
	6713.74	4.79	-1.52	22.0	7.57	22.5	7.57	23.6	7.58	15.6	7.42	22.4	7.58
	6716.25	4.58	-1.90	16.7	7.60	16.0	7.56	16.8	7.56	11.2	7.43	17.0	7.60

Table 2—Continued

Species	λ Å	χ eV	$\log gf$	EW(Sun) mÅ	$\log N$	EW(HIP71813) mÅ	$\log N$	EW(HIP76114) mÅ	$\log N$	EW(HIP77718) mÅ	$\log N$	EW(HIP78399)	$\log N$
	6725.36	4.10	-2.30	18.3	7.59	19.5	7.61	18.5	7.55	12.3	7.42	20.4	7.64
	6726.67	4.61	-1.12	48.5	7.54	49.2	7.56	48.4	7.50	37.3	7.38	52.4	7.61
	6733.15	4.64	-1.52	28.1	7.58	28.4	7.57	28.4	7.55	20.5	7.43	26.7	7.54
	6739.52	1.56	-4.98	12.8	7.58	13.4	7.57	12.9	7.50	8.1	7.42	12.7	7.56
	6745.98	4.07	-2.74	6.6	7.49	10.6	7.70	7.6	7.51	5.1	7.41	7.9	7.56
	6746.98	2.61	-4.35	3.8	7.42	5.6	7.53	2.8	7.33	4.6	7.49
	6750.16	2.42	-2.48	75.9	7.27	80.7	7.37	80.7	7.28	64.7	7.16	79.0	7.31
	6752.72	4.64	-1.30	37.7	7.55	38.5	7.56	39.1	7.54	27.6	7.39	38.1	7.55
Fe II	6239.95	3.89	-3.59	14.1	7.69	15.6	7.64	13.7	7.60	11.9	7.51	16.3	7.71
	6247.56	3.89	-2.55	54.8	7.68	56.3	7.62	51.7	7.54	55.5	7.62
	6385.46	5.55	-2.85	3.9	7.79	5.6	7.88	5.0	7.86	4.0	7.74	5.3	7.89
	6407.29	3.89	-3.49	33.3	8.14	35.9	8.10	33.9	8.07	25.2	7.85	34.6	8.10
	6446.40	6.22	-2.11	4.5	7.71	5.2	7.69	5.1	7.72	4.0	7.59	4.8	7.69
	6456.39	3.90	-2.25	64.0	7.57	65.9	7.53	63.5	7.48	60.6	7.43	69.6	7.62
	6506.36	5.59	-3.01	3.9	7.99	4.1	7.92	4.7	8.03	3.0	7.80	3.8	7.93
	6516.08	2.89	-3.55	55.3	7.70	59.7	7.70	55.9	7.62	52.7	7.57	57.8	7.68
Ni I	6767.78	1.83	-1.89	82.3	5.95	84.7	6.00	82.7	5.87	70.4	5.82	84.0	5.95
	6586.32	1.95	-2.95	44.4	6.44	43.3	6.38	45.7	6.38	29.6	6.19	40.7	6.34
	6598.61	4.23	-1.02	25.9	6.35	26.6	6.35	27.4	6.34	18.1	6.17	26.9	6.36
	6635.14	4.42	-0.87	24.5	6.35	25.8	6.36	25.1	6.32	17.6	6.18	24.0	6.32
	6643.64	1.68	-2.01	98.4	6.23	96.1	6.20	98.3	6.13	79.9	5.99	102.2	6.27
	6482.81	1.93	-2.97	41.3	6.38	42.0	6.36	43.1	6.34	28.8	6.18	40.5	6.34
	6532.88	1.93	-3.47	17.0	6.32	16.3	6.26	17.1	6.25	7.8	5.97	18.0	6.33

^aThe $\lambda 6300$ [O I] equivalent widths for all stars are presumed to contain a contribution from a blending Ni I feature that was accounted for as discussed in the text.

Table 3. Abundance Sensitivities

Species	ΔT_{eff} ± 100 K	$\Delta \log g$ ± 0.2 dex	$\Delta \xi$ ± 0.2 km s ⁻¹
Li I	± 0.09	± 0.02	∓ 0.00
O I	± 0.02	± 0.09	∓ 0.00
Al I	± 0.050	∓ 0.005	∓ 0.005
Ca I	± 0.067	∓ 0.016	∓ 0.033
Ti I	± 0.11	± 0.00	∓ 0.00
Fe I	± 0.070	± 0.005	∓ 0.023
Fe II	∓ 0.041	± 0.073	∓ 0.025
Ni I	± 0.073	± 0.013	∓ 0.039

Table 4. Solar Twin Candidate Summary

Parameter	Sun	HIP 71813 HD 129357	HIP 76114 HD 138573	HIP 77718 HD 142093	HIP 78399 HD 143436
M_V	4.83±0.01	4.45±0.11	4.77±0.06	4.83±0.07	4.87±0.10
$(B - V)^a$	0.642±0.004	0.644±0.002	0.661±0.005	0.604±0.007	0.644±0.001
$T_{\text{eff}}(\text{K})$	5777	5749±47	5710±50	5841±47	5768±43
ξ (km/s)	1.25	1.22±0.13	1.35±0.10	1.18±0.13	1.32±0.09
$[\text{m}/\text{H}]^b$	0.00	0.00	0.00	-0.15	0.00
$\log g$	4.44	4.16±0.13	4.20±0.15	4.33±0.15	4.28±0.12
$[\text{Fe}/\text{H}]$	0.	-0.02±0.04	-0.03±0.04	-0.15±0.04	-0.00±0.03
$[\text{Ni}/\text{H}]$	0.	-0.02±0.05	-0.06±0.05	-0.22±0.05	-0.02±0.04
$[\text{Ca}/\text{H}]$	0.	+0.02±0.04	-0.02±0.04	-0.09±0.04	+0.02±0.05
$[\text{Ti}/\text{H}]$	0.	+0.02±0.09	-0.06±0.08	-0.16±0.08	+0.02±0.07
$[\text{Al}/\text{H}]$	0.	-0.01±0.06	-0.04±0.05	-0.21±0.04	-0.07±0.04
$[\text{O}/\text{H}]$	0.	+0.03±0.10	+0.07±0.10	-0.51±0.19	-0.20±0.12
$\log N(\text{Li})$	1.03±0.04	≤0.6±0.04	0.8±0.13	2.27±0.06	1.79±0.07
$\log R_{\text{HK}}$	-4.95	-4.96	-5.00	-4.84	-4.87
$v \sin i$ (km/s)	≤2.5	≤2.5	≤2.1	≤2.8	≤2.6
M (M_{\odot}) ^c	1.01	1.00±0.06	0.97±0.015	0.975±0.015	1.01±0.02
Age (Gyr) ^c	4.2±0.2	8.2±1.3	7.8±2.0	5.0±2.3	3.8±2.9
U (km/s)		+21.3±1.5	-37.2±0.4	-5.6±0.3	-19.2±0.5
V (km/s)		-36.3±1.3	+9.0±0.4	-26.3±0.6	-38.6±1.6
W (km/s)		-32.0±0.4	-19.1±0.3	-16.9±0.2	-7.0±0.5

^aThe contentious solar color is taken from Cayrel de Strobel (1996).

^bThe metallicity characterizing the model atmosphere grids used in the abundance analysis.

^cMasses and ages derived from comparison of evolutionary tracks and position in the M_V vs. T_{eff} plane.